

Modeling and estimating mixed memberships in weighted networks

Huan Qing

QINGHUAN@CUMT.EDU.CN

School of Mathematics

China University of Mining and Technology

Xuzhou, 221116, P.R. China

Abstract

We consider the problem of detecting latent community information of mixed membership weighted network in which nodes have mixed memberships and edges connecting between nodes can be finite real numbers. We propose a general mixed membership distribution-free model for this problem. The model has no distribution constraints of edges but only the expected values, and can be viewed as generalizations of some previous models. We use an efficient spectral algorithm to estimate community memberships under the model. We also derive the convergence rate of the proposed algorithm under the model using spectral analysis. We demonstrate the advantages of mixed membership distribution-free model and the algorithm with applications to a small scale of simulated networks when edges follow different distributions. We have also applied the algorithm to five real world weighted network data sets with encouraging results.

Keywords: Communities, network models, overlapping community detection, weighted networks.

1. Introduction

For decades, the problem of community detection for networks has been actively studied in network science. The goal of community detection is to infer latent node's community information from the network, and community detection serves as a useful tool to learn network structure. The classical Stochastic Blockmodel (SBM) (Holland et al., 1983) models non-mixed un-weighted networks by assuming that the probability of an edge between two nodes depends on their respective communities and each node only belongs to one community. The Mixed Membership Stochastic Blockmodel (MMSB) Airoldi et al. (2008) extends SBM by allowing node to belong to multiple communities; models proposed in Karrer and Newman (2011); Jin et al. (2017); Zhang et al. (2020) extend SBM and MMSB by introducing node variation to model network in which node degree varies. Based on SBM and its extensions, substantial works on algorithms, applications and theoretical guarantees have been developed, to name a few, Rohe et al. (2011); Choi et al. (2011); Zhao et al. (2012); Lei and Rinaldo (2015); Abbe and Sandon (2015); Jin (2015); Joseph and Yu (2016); Abbe et al. (2016); Hajek et al. (2016); Gao et al. (2017); Chen et al. (2018); Zhou and A.Amini (2019); Wang et al. (2020); Mao et al. (2020).

However, the above models are built for un-weighted network and they can not model weighted network. To model weighted network in which node only belongs to one commu-

nity, some models which can be viewed as extensions of SBM are proposed Aicher et al. (2015); Jog and Loh (2015); Ahn et al. (2018); Palowitch et al. (2018); Xu et al. (2020); Ng and Murphy (2021); Qing (2021) in recent years. However, these models can not model weighted network in which node may belong to multiple communities (call such network as mixed membership weighted network). Especially, the Distribution-Free Models (DFM) of Qing (2021) can model weighted network without edge distribution constraint and allows spectral clustering to fit the model. Though the multi-way blockmodels proposed in Airoldi et al. (2013) can model mixed membership weighted network, it has a strong requirement on the distribution of edges such that edges must be random variables generated from Normal distribution. To model mixed membership weighted network, this article proposes a model based on a combination of the stochastic block idea of Holland et al. (1983), the mixed membership idea introduced in Airoldi et al. (2008) and the distribution-free idea introduced in Qing (2021).

The key contributions in this article are as follows: (1) We provide a general Mixed Membership Distribution-Free (MMDF for short) model to model mixed membership weighted network in which nodes may belong to multiple communities and edges can be any finite real numbers. MMDF does not require any prior knowledge on any specific distribution of network edges but only a expected value reflecting the community membership information, where the expected value is directly related with the structure of the proposed model. Especially, signed network with mixed memberships can be generated from MMDF. We also provide the identifiability of MMDF. Meanwhile, MMDF can be seen as extensions of some previous models such as SBM, MMSB and DFM. Detailed comparisons of our MMDF with some previous models for un-weighted network or weighted network can be found in next section. To the best of our knowledge, our MMDF is the first model for mixed membership weighted network in which edge can be generated from arbitrary distribution. (2) We use a spectral algorithm to fit MMDF, where the algorithm is designed based on the simplex structure inherent in the eigen-decomposition of adjacency matrix. The theoretical consistency of the proposed algorithm is built under MMDF. Especially, theoretical results when edges follow some distinct distributions can be immediately obtained from our results. When MMDF degenerates to SBM, we can obtain the classical separation condition of a standard network and this guarantees the optimality of our theoretical studies. (3) We study numerical performance of the proposed algorithm under MMDF when edges are generated from different distributions by changing some model parameters. The numerical results are consistent with our theoretical findings. We also apply the algorithm on five real world social weighted networks, and our data analysis results reveal the difference on network purity for different weighted networks.

Notations. We take the following general notations in this article. Write $[m] := \{1, 2, \dots, m\}$ for any positive integer m . For a vector x and fixed $q > 0$, $\|x\|_q$ denotes its l_q -norm, and we drop q for $\|x\|_q$ when q is 2. For a matrix M , M' denotes the transpose of the matrix M , $\|M\|$ denotes the spectral norm, $\|M\|_F$ denotes the Frobenius norm, $\|M\|_{2 \rightarrow \infty}$ denotes the maximum l_2 -norm of all the rows of M , and $\|M\|_\infty := \max_i \sum_j |M(i, j)|$ denotes the maximum absolute row sum of M . Let $\text{rank}(M)$ denote the rank of matrix M . Let $\sigma_i(M)$ be the i -th largest singular value of matrix M , $\lambda_i(M)$ denote the i -th largest eigenvalue of the matrix M ordered by the magnitude, and $\kappa(M)$ denote the condition number of M . $M(i, :)$ and $M(:, j)$ denote the i -th row and the j -th column of matrix M ,

respectively. $M(S_r, :)$ and $M(:, S_c)$ denote the rows and columns in the index sets S_r and S_c of matrix M , respectively. For any matrix M , we simply use $Y = \max(0, M)$ to represent $Y_{ij} = \max(0, M_{ij})$ for any i, j . $\mathbf{1}$ is a column vector with all entries being ones. e_i is the indicator vector with a 1 in entry i and 0 in all others.

2. The Mixed Membership Distribution-Free model

Consider an undirected weighted network \mathcal{N} with n nodes $\{1, 2, \dots, n\}$. Let $A \in \mathbb{R}^{n \times n}$ be the symmetric adjacency matrix of \mathcal{N} such that $A(i, j)$ denotes the weight between node i and node j for $i, j \in [n]$, and A is called adjacency matrix in this article. As a convention, we do not consider self edges, so A 's diagonal elements are 0. Note that $A(i, j)$ can be 0, 1, or some other finite real numbers since \mathcal{N} is a weighted network in this article. We assume all nodes in \mathcal{N} belong to K perceivable communities

$$\mathcal{C}^{(1)}, \mathcal{C}^{(2)}, \dots, \mathcal{C}^{(K)}. \quad (1)$$

Since we consider mixed membership weighted network in this article, node in \mathcal{N} may belong to multiple communities with different weights. Let $\Pi \in \mathbb{R}^{n \times K}$ be nodes membership matrix such that for $i \in [n], k \in [K]$,

$$\text{rank}(\Pi) = K, \Pi(i, k) \geq 0, \sum_{l=1}^K \Pi(i, l) = 1, \quad (2)$$

$$\text{Each of the } K \text{ communities has at least one pure node,} \quad (3)$$

where we call node i ‘pure’ if $\Pi(i, :)$ degenerates (i.e., one entry is 1, all others $K - 1$ entries are 0) and ‘mixed’ otherwise. In Eq (2), since $\Pi(i, k)$ is the weight of node i on community $\mathcal{C}^{(k)}$, $\|\Pi(i, :)\|_1 = 1$ means that $\Pi(i, :)$ is a $1 \times K$ probability mass function (PMF) for node i . Eq (3) is important for the identifiability of our model. For convenience, call Eq (3) pure nodes condition. For model modeling network with mixed memberships, pure nodes condition is significant for model identifiability, see models for un-weighted network with mixed memberships considered in Jin et al. (2017); Mao et al. (2020); Zhang et al. (2020). Let \mathcal{I} be the indices of nodes corresponding to K pure nodes, one from each community. Without loss of generality, let $\Pi(\mathcal{I}, :) = I_K$, where I_K is the $K \times K$ identity matrix.

Let the $K \times K$ connectivity matrix P satisfy

$$P = P', \text{rank}(P) = K, \text{and } \max_{k, l \in [K]} |P(k, l)| = 1. \quad (4)$$

We’d emphasize that P may have negative elements, the full rank requirement of P is mainly for the identifiability of our model, and we set the maximum absolute value of P 's entries as 1 mainly for convenience. Since P can have negative elements, it is not a matrix with probabilities unless \mathcal{F} is Bernoulli or Poisson or some other distributions. Meanwhile, unless specified, throughout this article, K is assumed to be a known integer.

Let $\rho > 0$ be a parameter that controls the sparsity of network \mathcal{N} , and call it sparsity parameter. For *arbitrary distribution* \mathcal{F} and all pairs of (i, j) with $i, j \in [n]$, our model constructs the adjacency matrix of the undirected weighted network \mathcal{N} such that $A(i, j)$ are independent random variables generated from \mathcal{F} with expectation

$$\mathbb{E}[A(i, j)] = \Omega(i, j), \text{ where } \Omega := \rho \Pi P \Pi'. \quad (5)$$

Call Ω population adjacency matrix in this article. Eq (5) means that we only assume all elements of A are independent random variables generated from arbitrary distribution \mathcal{F} with expectation $\Omega(i, j)$, without any prior knowledge on specific distribution of $A(i, j)$ for $i, j \in [n]$, and this guarantees that our model can model both weighted and un-weighted networks with mixed memberships. For comparison, mixed membership models considered in Airoldi et al. (2008); Zhang et al. (2020); Jin et al. (2017); Mao et al. (2018, 2020) require all entries of A are random variables from Bernoulli distribution with expectation $\Omega(i, j)$ since these models only model un-weighted network.

Definition 1 *Call equations (1)-(5) the Mixed Membership Distribution-Free (MMDF) model and denote it by $MMDF_n(K, P, \Pi, \rho)$.*

Next proposition which is distribution-free guarantees the identifiability of MMDF.

Proposition 1 *(Identifiability). MMDF is identifiable: For eligible (P, Π) and $(\tilde{P}, \tilde{\Pi})$, if $\rho\Pi\Pi\Pi' = \rho\tilde{\Pi}\tilde{P}\tilde{\Pi}'$, then $\Pi = \tilde{\Pi}$ and $P = \tilde{P}$.*

All proofs of proposition, lemmas and theorems are provided in the supplementary material in this paper. MMDF includes some previous models for community detection as special cases.

- Compared with the MMSB proposed in Airoldi et al. (2008), MMDF has no constraint on distribution \mathcal{F} and the distribution of Π while MMSB requires all entries of A follow Bernoulli distribution and Π follows Dirichlet distribution, and these increase the applicability of our model. Especially, MMSB limits all elements of P to being nonnegative while our MMDF allows P to have negative entries. To conclude, our MMDF can model both weighted and un-weighted networks while MMSB only models un-weighted networks.
- Compared with the model DFM, our MMDF reduces to DFM when all $\Pi(i, :)$ are degenerate, i.e., all nodes are pure. Thus, MMDF allows nodes to belong to multiple communities while DFM requires that each node belongs to a single community. Meanwhile, both MMDF and DFM can model weighted and un-weighted networks. To conclude, MMDF is a direct extension of DFM by allowing nodes to have mixed memberships, and the relationship between MMDF and DFM is similar as that of MMSB and SBM. Sure, our MMDF is also an extension of SBM since MMSB and DFM are extensions of SBM. It should be emphasized that though MMDF is an extension of DFM from non-mixed membership network to mixed membership network, it is at the cost of a stronger requirement on the rank of P for model's identifiability: MMDF's identifiability requires P to be full rank while DFM's identifiability allows P to be a singular matrix. And such phenomenon also occurs for MMSB and SBM.
- Compared with the weighted MMSB (WMMSB) of Dulac et al. (2020), our MMDF has no limit on distribution \mathcal{F} , distribution of Π , and allows P to have negative entries, while WMMSB requires that A follows Poisson distribution, Π follows Dirichlet distribution, and all entries of P are nonnegative. Our MMDF is more general than WMMSB.

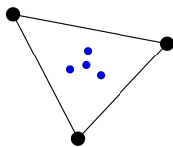


Figure 1: Rows of U : Ideal Simplex in Experiments 1-7 (black: pure nodes; blue: mixed nodes. Each point is a row of U . Many rows are equal by Lemma 1, so a point may denote many rows) of Section 5. K is 3, so there are three black points. Each PMF of mixed nodes belongs to 4 different PMFs, so there are 4 blue points. Since $K = 3$, for visualization, we have projected and rotated these points from \mathbb{R}^3 to \mathbb{R}^2 .

- Compared with weighted stochastic blockmodels (WSBM) in Aicher et al. (2015); Jog and Loh (2015); Ahn et al. (2018); Palowitch et al. (2018); Xu et al. (2020); Ng and Murphy (2021), these WSBM model weighted network in which every node only belong to one community, and they require all elements of P to be nonnegative or some distribution constraints on A , while our MMDF is distribution-free, models weighted network in which nodes enjoy mixed memberships, and allows P to have negative entries.

3. A spectral algorithm DFSP for fitting MMDF

The goal of community detection under model MMDF is to recover the membership matrix Π with network \mathcal{N} 's adjacency matrix A and the known number of communities K . To estimate Π with given A and K under MMDF, we start by providing an intuition on designing a spectral algorithm to fit model MMDF from the oracle case when Ω is known.

Since $\text{rank}(P) = K, \text{rank}(\Pi) = K, \text{rank}(\Omega) = K$ by basic algebra under $MMDF_n(K, P, \Pi, \rho)$. Let $\Omega = U\Lambda U'$ be the compact eigen-decomposition of Ω such that $U \in \mathbb{R}^{n \times K}, \Lambda \in \mathbb{R}^{K \times K}$, and $U'U = I_K$. The following lemma functions similar as Lemma 2.1 of Mao et al. (2020) and guarantees the existence of Ideal Simplex (IS for short), and the form $U = \Pi B$ is called IS when Π satisfies Eq (2)). It should be emphasized that the existence of IS is distribution-free as long as Π satisfies Eqs (2) and (3), and P is full rank.

Lemma 1 (*Ideal Simplex*). *Under $MMDF_n(K, P, \Pi, \rho)$, there exists an unique $K \times K$ matrix B such that $U = \Pi B$ where $B = U(\mathcal{I}, :)$.*

Figure 1 shows the IS by plotting rows of U under the settings in our simulations studies. We see that when i is pure node, $U(i, :)$ is the vertex of IS; otherwise, $U(i, :)$ is in the interior of the IS, and this is consistent with Lemma 1.

Given Ω and K , we can compute U immediately by top K eigen-decomposition of Ω . Then, once we can obtain $U(\mathcal{I}, :)$ from U , we can exactly recover Π by $\Pi = UU^{-1}(\mathcal{I}, :)$ since $U(\mathcal{I}, :) \in \mathbb{R}^{K \times K}$ is a full rank matrix based on Lemma 1. As suggested by Jin et al. (2017); Mao et al. (2020), for such IS, we can take the advantage of the successive projection (SP) algorithm proposed in Gillis and Vavasis (2015) (i.e., Algorithm 2) to U with K communities to exactly find the corner matrix $U(\mathcal{I}, :)$. For convenience, set $Z = UU^{-1}(\mathcal{I}, :)$. Since $\Pi = Z$,

we have $\Pi(i, :) = Z(i, :) \equiv \frac{Z(i, :)}{\|Z(i, :)\|_1}$ by the fact that $\|\Pi(i, :)\|_1 = 1$ for $i \in [n]$, where we write $\Pi(i, :) \equiv \frac{Z(i, :)}{\|Z(i, :)\|_1}$ mainly for the convenience to transfer the ideal algorithm given below to the real case.

The above gives rise to the following algorithm called Ideal DFSP (short for Distribution-Free SP algorithm), which is the ideal case of SPACL algorithm proposed in Mao et al. (2020). Input Ω, K . Output: Π .

- Let U be the top K eigenvectors with unit-norm of Ω .
- Run SP algorithm on all rows of U with K communities to obtain \mathcal{I} .
- Set $Z = UU^{-1}(\mathcal{I}, :)$.
- Recover Π by $\Pi(i, :) = Z(i, :)/\|Z(i, :)\|_1$ for $i \in [n]$.

Given U and K , since SP algorithm returns \mathcal{I} , we see that Ideal DFSP exactly returns Π , which supports the identifiability of MMDF in turn.

Next, we aim to extend the ideal case to the real case. The community membership matrix Π is unknown, and we aim at predicating it with given (A, K) when A is a random matrix generated from arbitrary distribution \mathcal{F} under MMDF. Let $\tilde{A} = \tilde{U}\tilde{\Lambda}\tilde{U}'$ be the top K eigen-decomposition of the adjacency matrix A such that $\tilde{U} \in \mathbb{R}^{n \times K}$, $\tilde{\Lambda} \in \mathbb{R}^{K \times K}$, $\tilde{U}'\tilde{U} = I_K$, and $\tilde{\Lambda}$ contains the leading K eigenvalues of A . Algorithm 1 called DFSP is a natural extension of the Ideal DFSP to the real case, and DFSP is the SPACL algorithm without the prune step of Mao et al. (2020), where we re-name it as DFSP to stress the distribution-free property of this algorithm.

Remark 1 *DFSP can also obtain assignments to non-overlapping communities by setting $\hat{c}_i = \arg \max_{1 \leq k \leq K} \hat{\Pi}(i, k)$ for $1 \leq i \leq n$, where \hat{c}_i is the community that node i belongs to.*

Algorithm 1 DFSP

Require: The adjacency matrix $A \in \mathbb{R}^{n \times n}$ and the number of communities K .

Ensure: The estimated $n \times K$ membership matrix $\hat{\Pi}$.

- 1: Compute $\tilde{A} = \tilde{U}\tilde{\Lambda}\tilde{U}'$, the top K eigen-decomposition of A .
 - 2: Run SP algorithm on all rows of \tilde{U} with K communities to obtain the estimated index set $\hat{\mathcal{I}}$ returned by SP.
 - 3: Set $\hat{Z} = \tilde{U}\tilde{U}^{-1}(\hat{\mathcal{I}}, :)$. Then set $\hat{Z} = \max(0, \hat{Z})$.
 - 4: Estimate $\Pi(i, :)$ by $\hat{\Pi}(i, :) = \hat{Z}(i, :)/\|\hat{Z}(i, :)\|_1, i \in [n]$.
-

4. Asymptotic consistency of DFSP under MMDF

In this section, we aim at proving that the estimated membership matrix $\hat{\Pi}$ returned by DFSP concentrate around Π when A is a random matrix generated under MMDF for any distribution F . We need the following two assumptions to control the variances of all entries of A and the sparsity of network \mathcal{N} .

Assumption 1 *Assume*

- $\tau = \max_{i,j \in [n]} |A(i,j) - \Omega(i,j)|$ is finite.
- $\gamma = \frac{\sigma_A^2}{\rho}$ is finite, where $\sigma_A^2 = \max_{i,j \in [n]} \text{Var}(A(i,j))$ and $\text{Var}(A(i,j))$ denotes the variance of $A(i,j)$.

Assumption 2 Assume $\gamma\rho n \geq \tau^2 \log(n)$.

As long as τ and γ are finite numbers, assumption 2 can be simplified as $\frac{\rho n}{\log(n)} \rightarrow \infty$ as $n \rightarrow \infty$, which means that though we allow the sparsity parameter ρ to go to zero as n goes to infinity, ρ should shrink slower than $\frac{\log(n)}{n}$, i.e., network \mathcal{N} can not be too sparse since ρ has a lower bound requirement $\frac{\log(n)}{n}$ when n increases. Here, the finiteness of τ and γ makes that we can let $\rho \rightarrow 0$ since ρ is a measure of network sparsity when all entries of A are nonnegative such as the cases when \mathcal{F} is Bernoulli or Binomial or Poisson distribution. Sure, if ρ is a constant, assumption 2 always hold for sufficiently large n . The finiteness of τ always holds since all entries of A and Ω are finite. After providing main result for DFSP algorithm under MMDF, we will use some examples to show that γ is always finite when setting \mathcal{F} as different distributions.

Similar as Jin et al. (2017); Mao et al. (2018, 2020), main theoretical results on bounds of errors for estimating mixed memberships rely on row-wise eigenspace error between the eigenvectors of adjacency matrix and eigenvectors of population adjacency matrix. With applications of Theorem 1.4 (the Matrix Bernstein) in Tropp (2012) and Theorem 4.2 in Cape et al. (2019) where this two theorems are distribution-free, next lemma provides upper bound of row-wise eigenspace error.

Lemma 2 (Row-wise eigenspace error) Under $MMDF_n(K, P, \Pi, \rho)$, when assumptions 1 and 2 hold, suppose $\sigma_K(\Omega) \geq C\sqrt{\gamma\rho n \log(n)}$ for some $C > 0$, with probability at least $1 - o(n^{-3})$, we have

$$\|\hat{U}\hat{U}' - UU'\|_{2 \rightarrow \infty} = O\left(\frac{\sqrt{\gamma n \log(n)}}{\sigma_K(P)\rho^{0.5}\lambda_K^{1.5}(\Pi'\Pi)}\right).$$

Though γ is assumed to be finite by assumption 1, we still let it enter the bound in Lemma 2 since it is directly related to the variances of A 's elements under distribution \mathcal{F} , i.e., only γ is related with distribution \mathcal{F} in our theoretical analysis though our model MMDF has no constraint on a specific distribution \mathcal{F} as long as Eq (5) holds. Meanwhile, we also benefit a lot from letting γ enter the theoretical bound when we aim at studying DFSP's performance under different distributions, and discussions given after Corollary 1 support this statement. Alternatively, Theorem 4.2. of Chen et al. (2021) can also be applied to obtain upper bound of $\|\hat{U}\hat{U}' - UU'\|_{2 \rightarrow \infty}$, and this bound is similar as the one in Lemma 2. For convenience, set $\varpi = \|\hat{U}\hat{U}' - UU'\|_{2 \rightarrow \infty}$. With an application of Lemma 2, next theorem provides theoretical upper bound on the l_1 errors of estimations for nodes memberships under MMDF.

Theorem 1 Under $MMDF_n(K, P, \Pi, \rho)$, let $\hat{\Pi}$ be obtained from DFSP algorithm, suppose conditions in Lemma 2 hold, there exists a permutation matrix $\mathcal{P} \in \mathbb{R}^{K \times K}$ such that with probability at least $1 - o(n^{-3})$, we have

$$\max_{i \in [n]} \|e_i'(\hat{\Pi} - \Pi\mathcal{P})\|_1 = O(\varpi \kappa(\Pi'\Pi) \sqrt{\lambda_1(\Pi'\Pi)}).$$

Since our model MMDF is distribution-free and \mathcal{F} can be arbitrary distribution as long as Eq (5) holds, Theorem 1 provides a general theoretical upper bound of the l_1 error between the estimated membership matrix $\hat{\Pi}$ and membership matrix Π up to a permutation of community labels under MMDF. Result in Theorem 1 can be simplified by adding some conditions on $\lambda_K(\Pi'\Pi)$ and K , as shown by the following corollary.

Corollary 1 *Under $MMDF_n(K, P, \Pi, \rho)$, when conditions of Lemma 2 hold, if we further suppose that $\lambda_K(\Pi'\Pi) = O(\frac{n}{K})$ and $K = O(1)$, with probability at least $1 - o(n^{-3})$, we have*

$$\max_{i \in [n]} \|e'_i(\hat{\Pi} - \Pi P)\|_1 = O\left(\frac{1}{\sigma_K(P)} \sqrt{\frac{\gamma \log(n)}{\rho n}}\right).$$

In Corollary 1, the condition $\lambda_K(\Pi'\Pi) = O(\frac{n}{K})$ means that summations of nodes weights in every community are in the same order, and $K = O(1)$ means that network \mathcal{N} has a constant number of communities. The concise form of bound in Corollary 1 is helpful for further analysis. When γ is finite, upper bound of error rate in Corollary 1 is $O(\frac{1}{\sigma_K(P)} \sqrt{\frac{\log(n)}{\rho n}})$. Thus, $\sigma_K(P)$ should shrink slower than $\sqrt{\frac{\log(n)}{\rho n}}$ for consistent estimation. If $\sigma_K(P)$ is a constant, ρ should shrink slower than $\frac{\log(n)}{n}$ for consistent estimation, and this matches assumption 2.

The following examples show that γ is finite under different distribution \mathcal{F} as long as Eq (5) holds.

- When $A(i, j) \sim \text{Normal}(\Omega(i, j), \sigma_A^2)$ for $i, j \in [n]$. When \mathcal{F} is Normal distribution, $\mathbb{E}[A(i, j)] = \Omega(i, j)$ holds by the property of Normal distribution, and P can have negative elements under MMDF. For this case, $\gamma = \frac{\sigma_A^2}{\rho}$, a finite number as long as $\sigma_A^2 \leq C\rho$ for some $C > 0$. Meanwhile, since γ is in the numerator position of the theoretical upper bound in Corollary 1, increasing σ_A^2 increases DFSP's error rate when $A(i, j) \sim \text{Normal}(\Omega(i, j), \sigma_A^2)$ for $i, j \in [n]$. Furthermore, setting γ as $\frac{\sigma_A^2}{\rho}$ in ϖ obtains theoretical upper bound of DFSP's l_1 error, and we see that increasing ρ decreases error. Finally, when \mathcal{F} is Normal distribution and Π is generated from Dirichlet distribution, our MMDF reduces to the multi-way blockmodels for undirected networks proposed in Airoldi et al. (2013).
- When $A(i, j) \sim \text{Binomial}(m, \frac{\Omega(i, j)}{m})$ for any positive integer m for $i, j \in [n]$. When \mathcal{F} is Binomial distribution, $\mathbb{E}[A(i, j)] = \Omega(i, j)$ holds by the property of Binomial distribution, and P should have nonnegative elements. Meanwhile, $\gamma = \max_{i, j \in [n]} m \frac{\Omega(i, j)}{m} (1 - \frac{\Omega(i, j)}{m}) / \rho \leq \max_{i, j \in [n]} \frac{\Omega(i, j)}{\rho} \leq 1$, i.e., γ is finite. Meanwhile, when Ω is fixed, increasing m increases γ , which gives a larger error rate. Sure, setting γ as 1 in ϖ obtains theoretical upper bound of DFSP's l_1 error.
- When $A(i, j) \sim \text{Bernoulli}(\Omega(i, j))$ for $i, j \in [n]$ and P is an nonnegative matrix such that MMDF reduces to MMSB. For this case, since $A(i, j) \sim \text{Bernoulli}(\Omega(i, j))$, we have $\mathbb{E}[A(i, j)] = \Omega(i, j)$, and $\text{Var}(A(i, j)) = \Omega(i, j)(1 - \Omega(i, j)) \leq \Omega(i, j) \leq \rho$, which suggests that $\gamma = 1$, a finite number.

- When $A(i, j) \sim \text{Poisson}(\Omega(i, j))$ for $i, j \in [n]$. By the property of Poisson distribution, $\mathbb{E}[A(i, j)] = \Omega(i, j)$ holds, and all entries of P should be nonnegative. Meanwhile, $\gamma = \max_{i, j \in [n]} \frac{\text{Var}(A(i, j))}{\rho} = \max_{i, j \in [n]} \frac{\Omega(i, j)}{\rho} \leq 1$, i.e., γ is finite. Meanwhile, the model DCSBM Karrer and Newman (2011) for non-mixed membership networks also let A 's elements follows Poisson distribution. For comparison, our MMDF lets A follow Poisson distribution and allows nodes to have mixed memberships.
- When $A(i, j) \sim \text{Laplace}(\Omega(i, j), \sigma_A/\sqrt{2})$ for $i, j \in [n]$. When \mathcal{F} is Laplace distribution, all elements of P are real values, $\mathbb{E}[A(i, j)] = \Omega(i, j)$ holds by the property of Laplace distributon, and $\text{Var}(A(i_r, j_c)) = \sigma_A^2$. Hence, γ is $\frac{\sigma_A^2}{\rho}$, a finite number.
- DCDFM can generate signed network by setting $\mathbb{P}(A(i, j) = 1) = \frac{1+\Omega(i, j)}{2}$ and $\mathbb{P}(A(i, j) = -1) = \frac{1-\Omega(i, j)}{2}$ (i.e., all non-diagonal entries of A are either 1 or -1). This case needs all elements of P be real values and $-1 \leq \Omega(i, j) \leq 1$. Then, we have $\mathbb{E}[A(i, j)] = \Omega(i, j)$, and $\text{Var}(A(i, j)) = 1 - \Omega^2(i, j) \leq 1$, i.e., $\gamma \leq \frac{1}{\rho}$ is finite.

The above examples show that γ is finite. Meanwhile, more than the above six distributions, the distribution-free property of MMDF allows \mathcal{F} to be other distributions as long as Eq (5) holds. For example, \mathcal{F} can be Double exponential, Exponential, Gamma, Laplace and Uniform distributions in <http://www.stat.rice.edu/~dobelman/courses/texts/distributions.c&b.pdf>. Details on probability mass function or probability density function on distributions discussed in this paper can also be found in the above url link. Generally speaking, the distribution-free property guarantees the generality of our model, our DFSP algorithm as well as our theoretical results.

We further consider a weighted network generated from MMDF when P is set as $P = \beta I_K + (1 - \beta)\mathbf{1}\mathbf{1}'$ for $\beta \in (0, 1]$ (note that $\sigma_K(P) = \beta$), $\lambda_K(\Pi'\Pi) = O(\frac{n}{K})$ and $K = O(1)$. Since $\Omega = \Pi\rho\Pi' = \Pi'\tilde{P}\Pi'$, where we set $\tilde{P} = \rho P$. Set $p_{\text{in}} = \rho, p_{\text{out}} = \rho(1 - \beta)$ (note that $p_{\text{in}} = \max_{k, l \in [K]} \tilde{P}(k, l)$, and $p_{\text{out}} = \min_{k, l \in [K]} \tilde{P}(k, l)$). By Corollary 1, the upper bound of error rate is $O(\frac{1}{\beta} \sqrt{\frac{\gamma \log(n)}{\rho n}})$, which suggests that increasing β decreases error rate. Meanwhile, to obtain consistent estimation, $\frac{p_{\text{in}} - p_{\text{out}}}{\sqrt{p_{\text{in}}}} = \beta\sqrt{\rho}$ should shrink slower than $\sqrt{\frac{\gamma \log(n)}{n}}$, and this threshold holds for any distribution \mathcal{F} under MMDF as long as Eq (5) holds. Especially, when \mathcal{F} is Bernoulli distribution and all nodes are pure such that MMDF reduces to SBM, the above threshold is the classical separation condition in Corollary 1 of McSherry (2001) since γ is 1 for Bernoulli distribution, and this guarantees the optimality of our theoretical results.

5. Simulations

In this section, we study DFSP's performance over a series of simulations when A is generated under MMDF for different distribution \mathcal{F} . We measure the performance of DFSP by the following error rate:

$$\min_{\mathcal{P} \in \{K \times K \text{ permutation matrix}\}} \frac{1}{n} \|\hat{\Pi} - \Pi\mathcal{P}\|_1.$$

For all simulations, unless specified, set $n = 200$, $K = 3$, and $n_0 = 40$, where n_0 denotes the number of pure nodes for each community. Let all mixed nodes have four different memberships $(0.4, 0.4, 0.2)$, $(0.4, 0.2, 0.4)$, $(0.2, 0.4, 0.4)$ and $(1/3, 1/3, 1/3)$, each with $\frac{n-3n_0}{4}$ number of nodes. The connectivity matrix P and sparsity parameter ρ are set independently for each experiment. Note that maximum entries of ρP are allowed to be larger than 1 under MMDF when F is not Bernoulli distribution because entries of ρP are not probabilities when F is not Bernoulli. Meanwhile, in all numerical studies, the only criteria for choosing P is, P should obey Eq (4), and P 's entries should be positive or negative relying on \mathcal{F} . Each simulation experiment contains the following steps:

- (a) Set $\Omega = \rho \Pi P \Pi'$.
- (b) Let $A(i, j)$ be a random number generated from distribution \mathcal{F} with expectation $\Omega(i, j)$ for $1 \leq i < j \leq n$, set $A(j, i) = A(i, j)$ to make A be symmetric, and let A 's diagonal elements be zero since we do not consider self-edges.
- (c) Apply DFSP to A with K communities. Record error rate.
- (d) Repeat (b)-(c) for 50 times, and report the averaged error rates over the 50 repetitions.

Experiment 1: Normal distribution. Set \mathcal{F} as Normal distribution such that $A(i, j) \sim \text{Normal}(\Omega(i, j), \sigma_A^2)$ for some σ_A^2 . Set P as

$$P = \begin{bmatrix} -1 & -0.2 & 0.3 \\ -0.2 & 0.9 & 0.3 \\ 0.3 & 0.3 & 0.9 \end{bmatrix}.$$

Note that when \mathcal{F} is Normal distribution, P is allowed to have negative entries and A can have negative elements under MMDF. This experiment has two sub-experiments.

Experiment 1[a]. Let $\sigma_A^2 = 2$, and ρ range in $\{0.1, 0.2, \dots, 2\}$. The results are presented in Panel (a) of Figure 2. We see that DFSP performs better as ρ increases, and this is consistent with our Corollary 1. Meanwhile, we also plot \hat{U} in Panels (a), (b) and (c) of Figure 4 for different ρ when σ_A^2 is fixed, where we see the estimated simplex obtained from \hat{U} when applying SP algorithm is more “close” to the Ideal Simplex in Figure 1 when increasing ρ , and this explains why DFSP performs better when ρ increases.

Experiment 1[b]. Let $\rho = 0.5$, and σ_A^2 range in $\{0.1, 0.2, \dots, 2\}$. The results are presented in Panel (b) of Figure 2, and we find that DFSP performs poorer as σ_A^2 increases which matches the 1st bullet given after Corollary 1. Panels (d), (e) and (f) of Figure 4 show plots of \hat{U} for different σ_A^2 when ρ is fixed, and the three panels show that the estimated simplex obtained from \hat{U} is more “farther” to the Ideal Simplex in Figure 1 when increasing σ_A^2 , and this explains why DFSP performs poorer when σ_A^2 increases.

Experiment 2: Binomial distribution. Set \mathcal{F} as Binomial distribution such that $A(i, j) \sim \text{Binomial}(m, \frac{\Omega(i, j)}{m})$ for some positive integer m . Note that, since $\Omega(i, j) \leq \rho$ and $\frac{\Omega(i, j)}{m}$ is probability for all nodes, ρ should be set smaller than m in this experiment. Meanwhile, when \mathcal{F} is Binomial, elements of A take values from $\{0, 1, 2, \dots, m\}$. Set P as

$$P = \begin{bmatrix} 1 & 0.2 & 0.3 \\ 0.2 & 0.9 & 0.3 \\ 0.3 & 0.3 & 0.9 \end{bmatrix}.$$

This experiment has two sub-experiments.

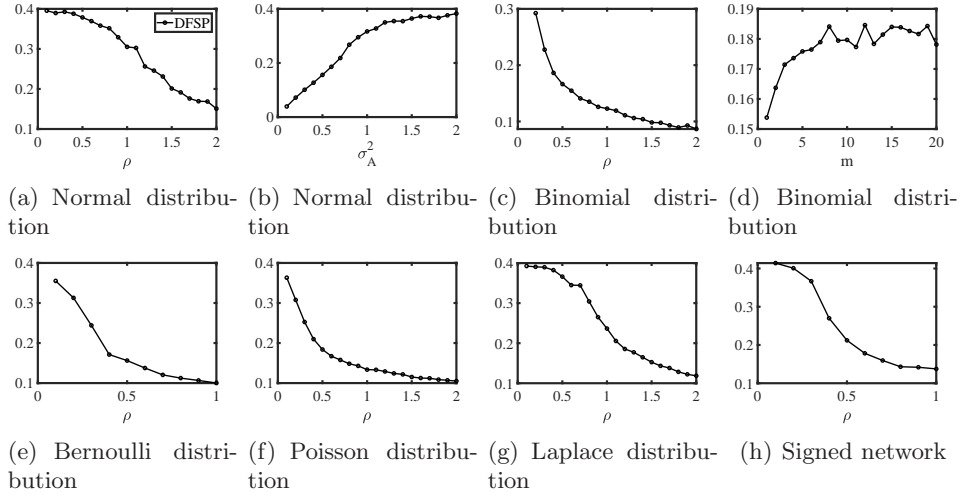


Figure 2: Numerical results of Experiments 1-6. y-axis: error rate.

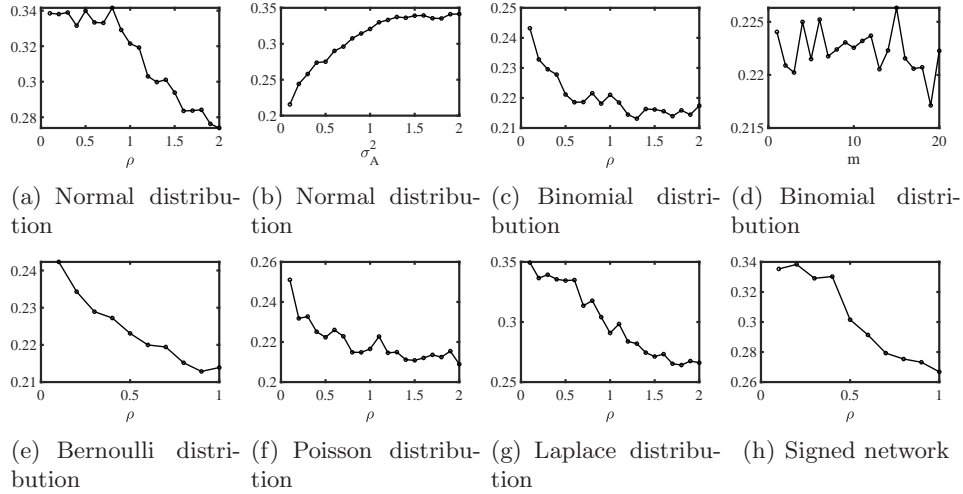


Figure 3: Numerical results of Experiments 1-6 without pure nodes: the six panels are plotted under the same settings as panels (a)-(h) of Figure 2 except that $n_0 = 0$ (i.e., no pure node for each community), a case for DFSP’s sensitivity on MMDF’s pure nodes condition. Compared with error rates in Figure 2, though DFSP performs slightly poorer, it still can estimate memberships even when there is no pure nodes which suggests that DFSP is not sensitive on MMDF’s pure nodes condition. y-axis: error rate.

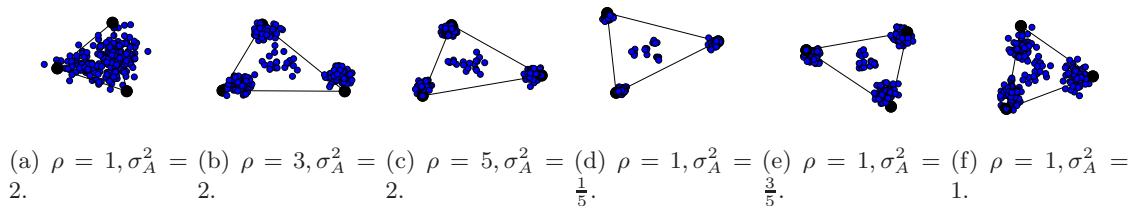


Figure 4: Normal distribution: \hat{U} . Each point is a row of \hat{U} , and the three black points represent the three rows of $\hat{U}(\hat{\mathcal{I}}, :)$, where $\hat{\mathcal{I}}$ is estimated index set returned by SP. Since $K = 3$, for visualization, we have projected and rotated these points from \mathbb{R}^3 to \mathbb{R}^2 .

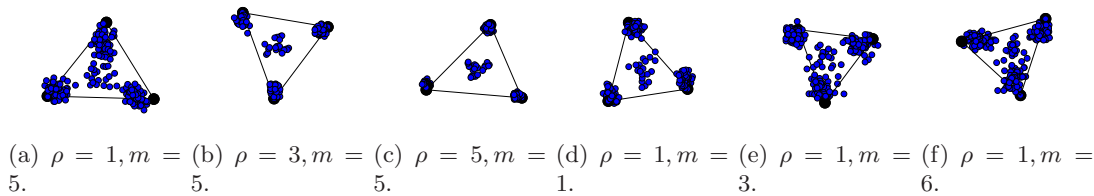


Figure 5: Binomial distribution: \hat{U} .

Experiment 2[a]. Let $m = 4$, and ρ range in $\{0.1, 0.2, \dots, 2\}$. Results are shown in Panel (c) of Figure 2, and we see that DFSP enjoys better performance as ρ increases when \mathcal{F} is Binomial distribution. Meanwhile, panels (a), (b) and (c) of Figure 5 show plots of \hat{U} when changing ρ . We see that a more clear structure of simplex appears as ρ increases, thus a easier case for DFSP to recover nodes memberships.

Experiment 2[b]. Let $\rho = 0.5$, and m range in $\{1, 2, \dots, 20\}$. Panel (d) of Figure 2 displays the results. It suggests that increasing m increases error rate of DFSP, and this is consistent with theoretical findings in the 2nd bullet given after Corollary 1. Meanwhile, we also plot \hat{U} for different m when ρ is fixed in Figure 5. We see that the estimated simplex obtained from \hat{U} via applying SP algorithm is farther to the Ideal Simplex when m increases, creating a harder case for DFSP to recover Π .

Experiment 3: Bernoulli distribution. Set \mathcal{F} as Bernoulli distribution such that $A(i, j) \sim \text{Bernoulli}(\Omega(i, j))$. Set P same as Experiment 2. Meanwhile, for the Bernoulli case, all entries of A are either 0 or 1. Let ρ range in $\{0.1, 0.2, \dots, 1\}$. Panel (e) of Figure

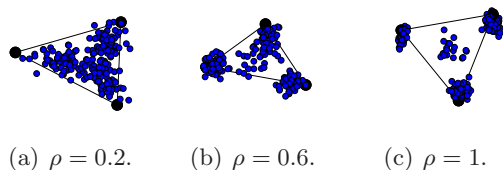
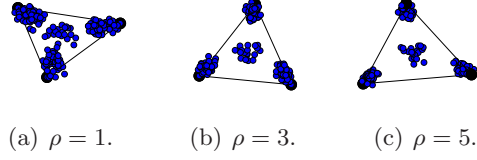
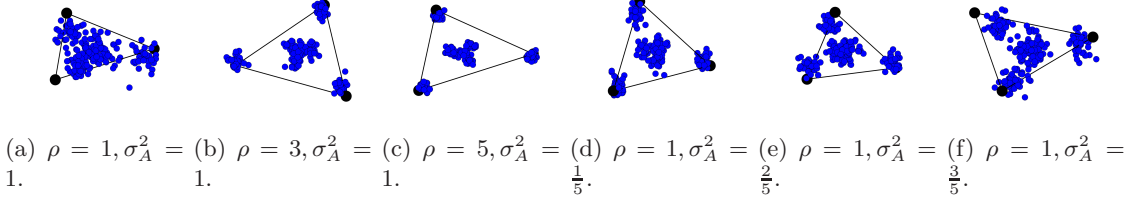


Figure 6: Bernoulli distribution: \hat{U} .


 Figure 7: Poisson distribution: \hat{U} .

 Figure 8: Laplace distribution: \hat{U} .

2 shows the results. Similarly, we can plot \hat{U} for this Experiment 3 (also for Experiments 4, 5 and 6) by changing ρ as Experiments 1 and 2, and Figure 6 displays plots of \hat{U} .

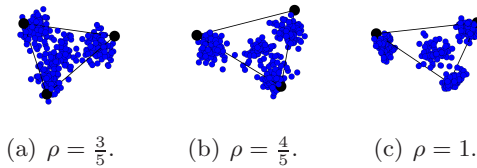
Experiment 4: Poisson distribution. Set \mathcal{F} as Poisson distribution such that $A(i, j) \sim \text{Poisson}(\Omega(i, j))$. Set P same as Experiment 2. For Poisson distribution, all entries of A take values from $\{0, 1, 2, \dots\}$. Let ρ range in $\{0.1, 0.2, \dots, 2\}$. Panel (f) of Figure 2 displays the results.

Experiment 5: Laplace distribution. Set \mathcal{F} as Laplace distribution such that $A(i, j) \sim \text{Laplace}(\Omega(i, j), \sigma_A/\sqrt{2})$. Set $\sigma_A = 1$, and P same as Experiment 1. Let ρ range in $\{0.1, 0.2, \dots, 2\}$. Panel (g) of Figure 2 displays the results.

Experiment 6: Signed network. For signed network when $\mathbb{P}(A(i, j) = 1) = \frac{1+\Omega(i, j)}{2}$ and $\mathbb{P}(A(i, j) = -1) = \frac{1-\Omega(i, j)}{2}$, let $n = 300$, each community own $n_0 = 80$ number of pure nodes, all mixed nodes's memberships and P be the same as that of Experiment 1. Let ρ range in $\{0.1, 0.2, \dots, 1\}$. Panel (h) of Figure 2 displays the results.

Experiment 7: Changing β . Let $\beta \in \{0.1, 0.2, \dots, 1\}$. Set $\rho = 1$, and P as

$$P = \begin{bmatrix} 1 & 1 - \beta & 1 - \beta \\ 1 - \beta & 1 & 1 - \beta \\ 1 - \beta & 1 - \beta & 1 \end{bmatrix}.$$


 Figure 9: Signed network: \hat{U} .

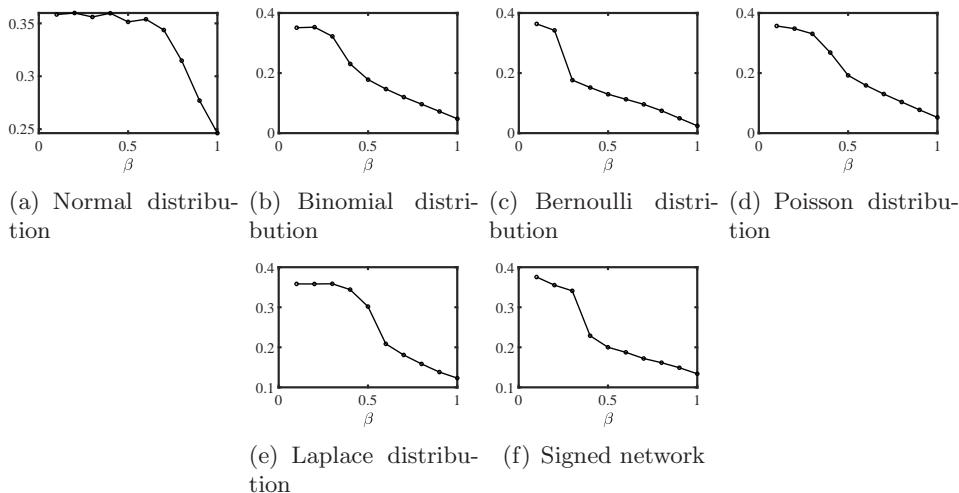


Figure 10: Numerical results of Experiment 7. y-axis: error rate.

Since $\sigma_K(P) = \beta$, increasing β decreases error rate by the analysis given after Corollary 1. This experiment has six sub-experiments.

Experiment 7 [a]. Let \mathcal{F} be Normal distribution such that $A(i, j) \sim \text{Normal}(\Omega(i, j), 2)$.

Experiment 7 [b]. Let \mathcal{F} be Binomial distribution such that $A(i, j) \sim \text{Binomial}(4, \frac{\Omega(i, j)}{4})$.

Experiment 7 [c]. Let \mathcal{F} be Bernoulli distribution such that $A(i, j) \sim \text{Bernoulli}(\Omega(i, j))$.

Experiment 7 [d]. Let \mathcal{F} be Poisson distribution such that $A(i, j) \sim \text{Poisson}(\Omega(i, j))$.

Experiment 7 [e]. Let \mathcal{F} be Laplace distribution such that $A(i, j) \sim \text{Laplace}(\Omega(i, j), 1)$.

Experiment 7 [f]. Let \mathcal{F} be distribution of signed network such that $\mathbb{P}(A(i, j) = 1) = \frac{1 + \Omega(i, j)}{2}$ and $\mathbb{P}(A(i, j) = -1) = \frac{1 - \Omega(i, j)}{2}$.

The results of Experiment 7 are displayed Figure 10. It suggests that DFSP performs better when β increases, and this supports our theoretical findings given after Corollary 1.

6. Application to real world weighted networks

Recall that the $K \times 1$ vector $\hat{\Pi}(i, :)$ is the estimated membership for node $i \in [n]$, we need the following definition.

Definition 2 For a constant $\zeta \in [0.6, 1)$, let $\varphi(\zeta) = \frac{|\{i \in [n]: \hat{\Pi}_{i, \max} \geq \zeta\}|}{n}$, where $\hat{\Pi}_{i, \max} = \max_{1 \leq k \leq K} \hat{\Pi}(i, k)$. Call $\varphi(\zeta)$ the network purity, ζ the purity threshold, and $\hat{\Pi}_{i, \max}$ the purity of node i .

In the definition of purity, node i is regarded as a highly pure node if $\hat{\Pi}_{i, \max} \geq \zeta$, thus $\varphi(\zeta)$ represents the proportion of highly pure nodes and it is useful in investigating the purity of real world weighted networks. Sure, increasing ζ increases the requirement on network purity.

We apply DFSP to five real world weighted networks, Gahuku-Gama subtribes Read (1954), Karate-club-weighted Zachary (1977), Coauthorships in network science (Coauthorships for short) Newman (2006), Condensed matter collaborations 1999 (Con-mat-1999 for short) Newman (2001), and Condensed matter collaborations 2003 (Con-mat-2003 for

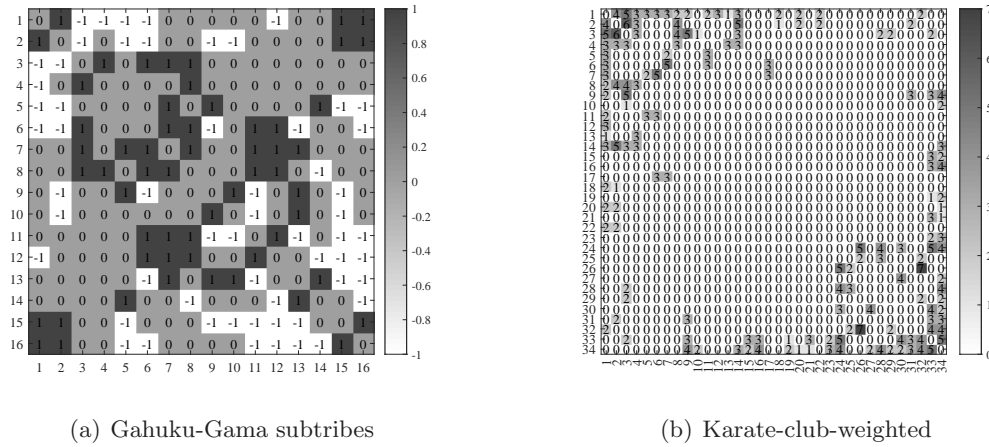


Figure 11: Adjacency matrices of Gahuku-Gama subtribes and Karate-club-weighted.

short) Newman (2001). For visualization, Figure 11 shows adjacency matrices of the first two weighted networks, and we see that all edge weights for Karate-club-weighted network are nonnegative and Gahuku-Gama subtribes is a signed network. For the other three networks, all edge weights are nonnegative. Table 1 summaries basic information for these networks. Brief introduction on these networks are given below.

Gahuku-Gama subtribes: This data is the signed social network of tribes of the Gahuku–Gama alliance structure of the Eastern Central Highlands of New Guinea Kunegis (2013). Positive link means alliance while negative link means enmity. Meanwhile, this network has 3 communities, its nodes labels shown in Figure 9 (b) from Yang et al. (2007) are regarded as ground truth here. This data can be downloaded from <http://konect.cc/>.

Karate-club-weighted: In this network, node means member of a karate club in a university, and edge denotes the relative strength of associations. This network is the weighted version of the classical Karate club network. So, the number of communities is 2 and true labels for all members are known for Karate-weighted. This data can be downloaded from <http://vlado.fmf.uni-lj.si/pub/networks/data/ucinet/ucidata.htm#kazalo>, and the classical Karate club network and its true labels can be found in <http://www-personal.umich.edu/~me>

Coauthorships: This data can be downloaded from <http://www-personal.umich.edu/~mejn/netdata/>. In this network, node denotes scientist and weights provided by the original papers mean coauthorship. The original network has 1589 nodes, and only 379 nodes fall in the largest connected component, and we focus on the giant component in this paper. To find K , we plot the leading 20 singular values of its adjacency matrix. Results shown in Figure 12 suggest that K is 2.

Con-mat-1999: This data can be downloaded from <http://www-personal.umich.edu/~mejn/netdata/>. It is a weighted network of coauthorships between scientists posting preprints on the Condensed Matter E-Print Archive between Jan 1, 1995 and December 31, 1999. Edge weights are provided by the original papers. The original network has 16726 nodes, and its largest connected component which we study in this paper has 13861 nodes. Eigen-gap shown in Figure 12 suggests that K is 2 for this network.

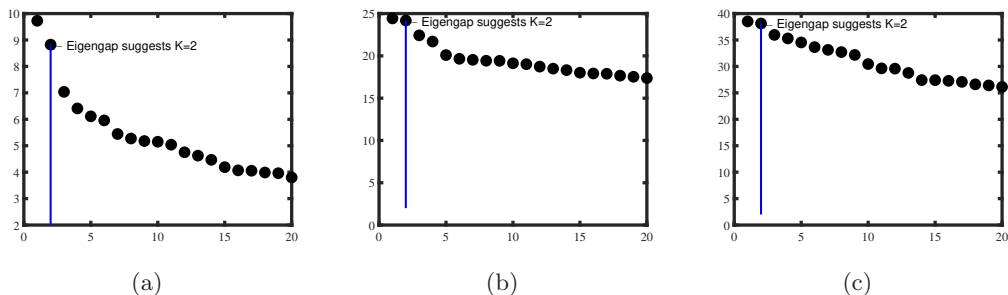


Figure 12: Panels (a),(b) and (c) show leading 20 singular values of adjacency matrices for Coauthorships, Cond-mat-1999 and Cond-mat-2003, respectively.

Con-mat-2003: It is updated network of Con-mat-1999. This network has 31163 nodes, and the largest connected component used in this paper has 27519 nodes. Eigen-gap shown in Figure 12 also suggests that K is 2 for Con-mat-2003.

Table 1: Five real world weighted networks.

| | n | K | $\max_{i,j} A(i, j)$ | $\min_{i,j} A(i, j)$ | #Edges | %Positive edges |
|-----------------------|-------|---------|----------------------|----------------------|--------|-----------------|
| Gahuku-Gama subtribes | 16 | 3 | 1 | -1 | 58 | 50% |
| Karate-club-weighted | 34 | 2 | 7 | 0 | 78 | 100% |
| Coauthorships | 379 | Unknown | 4.75 | 0 | 914 | 100% |
| Con-mat-1999 | 13861 | Unknown | 22.3333 | 0 | 44619 | 100% |
| Con-mat-2003 | 27519 | Unknown | 35.2 | 0 | 116181 | 100% |

Let $\hat{\Pi}$ be the estimated membership matrix returned by applying DFSP on Gahuku-Gama subtribes network with 3 communities, and set $\hat{c}_i = \arg \max_{1 \leq k \leq K} \hat{\Pi}(i, k)$ for $1 \leq i \leq n$ as the estimated label for node i . By comparing \hat{c} with the true labels for Gahuku-Gama subtribes network, we find that DFSP misclusters 0 nodes out of 16. Similarly, applying DFSP on Karate-club-weighted network with 2 communities obtains estimated labels for all nodes, and we find that DFSP misclusters 0 nodes out of 34.

Since true membership matrix is unknown for Coauthorships network, we apply DFSP to this data with two clusters to obtain estimated membership matrix $\hat{\Pi}$, and then computing network purity for different choices of the purity threshold ζ based on $\hat{\Pi}$. True membership matrix is also unknown for Con-mat-1999 (and Con-mat-2003) network, and we also compute its purity. Meanwhile, for comparison, we provide purity of Gahuku-Gama subtribes and Karate-club-weighted networks. The results are displayed in Table 2. We see that (1) $\phi(0.9)$ for Gahuku-Gama subtribes is 0.8750, which is quite small compared with 1, thus this network has $16 - 16\phi(0.9) = 2$ highly mixed nodes for a large purity threshold 0.9. (2) for Karate-club weighted network, it has $34 - 34\phi(0.85) \approx 4$ highly mixed nodes for purity threshold 0.85, $34 - 34\phi(0.9) \approx 7$ highly mixed nodes for a large purity threshold 0.9. Purity of Katate-club-weighted network is smaller than that of Gahuku-Gama subtribes network for a same purity threshold ζ , thus Katate-club-weighted is more mixed than Gahuku-Gama subtribes. (3) for Coauthorships network, it has $379 - 379\phi(0.85) \approx 9$ highly mixed nodes when $\zeta = 0.85$, and $379 - 379\phi(0.9) \approx 23$ highly mixed nodes when

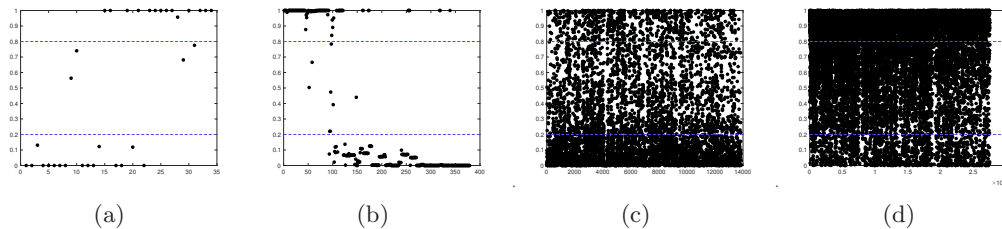


Figure 13: Panels (a)-(d): $\hat{\Pi}(:, 1)$ for Karate-club-weighted, Coauthorships, Con-mat-1999 and Con-mat-2003, respectively. Recall that K is 2 for the four networks, $\hat{\Pi}(i, 1)$ is the estimated probability that node i belongs to community 1, for $i \in [n]$. We believe that a node is highly mixed if it falls between the two blue dash lines (a case for purity threshold 0.8).

$\zeta = 0.9$. Compared with Gahuku-Gama subtribes and Karate-club-weighted, we see that Coauthorships is a highly pure network since its purity is always larger than Gahuku-Gama subtribes and Karate-club-weighted for the same purity threshold. (4) for Con-mat-1999, it has $13861 - 13861 * \phi(0.7) = 2039$ highly mixed nodes for a small purity threshold 0.7. Con-mat-1999 is a highly mixed network since its purity is always smaller than that of Gahuku-Gama subtribes, Karate-club-weighted and Coauthorships for a same purity threshold. Similar arguments hold for Con-mat-2003, and we find that Con-mat-2003 is more mixed than the other four networks. Meanwhile, for a direct observation on network purity, we plot $\hat{\Pi}(:, 1)$ in Figure 13 for Karate-club-weighted, Coauthorships, Con-mat-1999 and Con-mat-2003 networks since the number of communities is 2 for the four networks and $\hat{\Pi}(i, 1)$ is the estimated probability that node i belongs to community 1. We see that for Karate-club-weighted and Coauthorships, the proportions of nodes falling between the two blue dash lines are much smaller than that of Con-mat-1999 and Con-mat-2003, which means that Con-mat-1999 and Con-mat-2003 are highly mixed networks.

Table 2: Purity for the five network data sets in Table 1 when varying threshold ζ .

| | Gahuku-Gama subtribes | Karate-club-weighted | Coauthorships | Con-mat-1999 | Con-mat-2003 |
|-----------------|-----------------------|----------------------|---------------|--------------|--------------|
| $\varphi(0.7)$ | 0.9375 | 0.9412 | 0.9868 | 0.8529 | 0.7780 |
| $\varphi(0.75)$ | 0.9375 | 0.9118 | 0.9868 | 0.8003 | 0.7034 |
| $\varphi(0.8)$ | 0.9375 | 0.8824 | 0.9789 | 0.7404 | 0.6336 |
| $\varphi(0.85)$ | 0.9375 | 0.8824 | 0.9763 | 0.6723 | 0.5502 |
| $\varphi(0.9)$ | 0.8750 | 0.7941 | 0.9393 | 0.5777 | 0.4470 |

7. Conclusion

In this article, we introduce a general, flexible and identifiable mixed membership distribution-free model, which is, to the best of our knowledge, the first model for mixed membership weighted network in which edges can be generated from arbitrary distribution as long as Eq (5) holds, where Eq (5) is directly related with the latent community information. The distribution-free property of the proposed model even allows elements of adjacency ma-

trix to be any finite real value. The model provides exploratory tools for studying latent structural information of network in which nodes belong to multiple communities and edges can be generated from any distribution. An efficient spectral algorithm designed based on the simplex structure inherent in the eigenvectors of the population adjacency matrix is applied to fit the model. We show the estimation consistency of the algorithm under our model by considering network sparsity and taking the advantage of recent technique on row-wise eigenvectors deviation. Our theoretic framework on consistent estimation also enjoys distribution-free property such that results when edges follow different distributions can be obtained immediately. Numerical results obtained by applying the algorithm to detect community membership of various simulated mixed membership weighted networks when edges are generated from different distributions under the model are consistent with the theoretical results. Numerical results on real world social weighted networks reveal the difference on network purity. We expect that the mixed membership distribution-free model and the algorithm fitting the model proposed in this article will have wide applications on learning and understanding latent structure of mixed membership weighted network in network science.

References

- Emmanuel Abbe and Colin Sandon. Community detection in general stochastic block models: Fundamental limits and efficient algorithms for recovery. In *2015 IEEE 56th Annual Symposium on Foundations of Computer Science*, pages 670–688, 2015.
- Emmanuel Abbe, Afonso S. Bandeira, and Georgina Hall. Exact recovery in the stochastic block model. *IEEE Transactions on Information Theory*, 62(1):471–487, 2016.
- Kwangjun Ahn, Kangwook Lee, and Changho Suh. Hypergraph spectral clustering in the weighted stochastic block model. *IEEE Journal of Selected Topics in Signal Processing*, 12(5):959–974, 2018.
- Christopher Aicher, Abigail Z. Jacobs, and Aaron Clauset. Learning latent block structure in weighted networks. *Journal of Complex Networks*, 3(2):221–248, 2015.
- Edoardo M. Airoldi, David M. Blei, Stephen E. Fienberg, and Eric P. Xing. Mixed membership stochastic blockmodels. *Journal of Machine Learning Research*, 9:1981–2014, 2008.
- Edoardo M. Airoldi, Xiaopei Wang, and Xiaodong Lin. Multi-way blockmodels for analyzing coordinated high-dimensional responses. *The Annals of Applied Statistics*, 7(4):2431–2457, 2013.
- Joshua Cape, Minh Tang, and Carey E. Priebe. The two-to-infinity norm and singular subspace geometry with applications to high-dimensional statistics. *Annals of Statistics*, 47(5):2405–2439, 2019.
- Yudong Chen, Xiaodong Li, and Jiaming Xu. Convexified modularity maximization for degree-corrected stochastic block models. *Annals of Statistics*, 46(4):1573–1602, 2018.

- Yuxin Chen, Yuejie Chi, Jianqing Fan, and Cong Ma. Spectral methods for data science: A statistical perspective. *Foundations and Trends® in Machine Learning*, 14(5):566–806, 2021.
- David S. Choi, Patrick J. Wolfe, and Edoardo M. Airoldi. Stochastic blockmodels with a growing number of classes. *Biometrika*, 99(2):273–284, 2011.
- Adrien Dulac, Eric Gaussier, and Christine Largeton. Mixed-membership stochastic block models for weighted networks. In *Conference on Uncertainty in Artificial Intelligence (UAI)*, volume 124, pages 679–688, 2020.
- Chao Gao, Zongming Ma, Anderson Y. Zhang, and Harrison H. Zhou. Achieving optimal misclassification proportion in stochastic block models. *Journal of Machine Learning Research*, 18(60):1–45, 2017.
- Nicolas Gillis and Stephen A. Vavasis. Semidefinite programming based preconditioning for more robust near-separable nonnegative matrix factorization. *SIAM Journal on Optimization*, 25(1):677–698, 2015.
- Bruce Hajek, Yihong Wu, and Jiaming Xu. Achieving exact cluster recovery threshold via semidefinite programming. *IEEE Transactions on Information Theory*, 62(5):2788–2797, 2016.
- Paul W. Holland, Kathryn Blackmond Laskey, and Samuel Leinhardt. Stochastic block-models: First steps. *Social Networks*, 5(2):109–137, 1983.
- Jiashun Jin. Fast community detection by SCORE. *Annals of Statistics*, 43(1):57–89, 2015.
- Jiashun Jin, Zheng Tracy Ke, and Shengming Luo. Estimating network memberships by simplex vertex hunting. *arXiv: Methodology*, 2017.
- Varun Jog and Po-Ling Loh. Information-theoretic bounds for exact recovery in weighted stochastic block models using the renyi divergence, 2015.
- Antony Joseph and Bin Yu. Impact of regularization on spectral clustering. *Annals of Statistics*, 44(4):1765–1791, 2016.
- Brian Karrer and M. E. J. Newman. Stochastic blockmodels and community structure in networks. *Physical Review E*, 83(1):16107, 2011.
- Jérôme Kunegis. Konect: the koblenz network collection. In *Proceedings of the 22nd international conference on world wide web*, pages 1343–1350, 2013.
- Jing Lei and Alessandro Rinaldo. Consistency of spectral clustering in stochastic block models. *Annals of Statistics*, 43(1):215–237, 2015.
- Xueyu Mao, Purnamrita Sarkar, and Deepayan Chakrabarti. Overlapping clustering models, and one (class) svm to bind them all. In *Advances in Neural Information Processing Systems*, volume 31, pages 2126–2136, 2018.

- Xueyu Mao, Purnamrita Sarkar, and Deepayan Chakrabarti. Estimating mixed memberships with sharp eigenvector deviations. *Journal of the American Statistical Association*, pages 1–13, 2020.
- F. McSherry. Spectral partitioning of random graphs. In *Proceedings 2001 IEEE International Conference on Cluster Computing*, pages 529–537, 2001.
- Mark EJ Newman. The structure of scientific collaboration networks. *Proceedings of the national academy of sciences*, 98(2):404–409, 2001.
- Mark EJ Newman. Finding community structure in networks using the eigenvectors of matrices. *Physical review E*, 74(3):036104, 2006.
- Tin Lok James Ng and Thomas Brendan Murphy. Weighted stochastic block model. *Statistical Methods and Applications*, 2021.
- John Palowitch, Shankar Bhamidi, and Andrew B. Nobel. Significance-based community detection in weighted networks. *Journal of Machine Learning Research*, 18(188):1–48, 2018.
- Huan Qing. Distribution-free models for community detection. *arXiv preprint arXiv:2111.07495*, 2021.
- Kenneth E Read. Cultures of the central highlands, new guinea. *Southwestern Journal of Anthropology*, 10(1):1–43, 1954.
- Karl Rohe, Sourav Chatterjee, and Bin Yu. Spectral clustering and the high-dimensional stochastic blockmodel. *Annals of Statistics*, 39(4):1878–1915, 2011.
- Joel A. Tropp. User-friendly tail bounds for sums of random matrices. *Foundations of Computational Mathematics*, 12(4):389–434, 2012.
- Zhe. Wang, Yingbin. Liang, and Pengsheng. Ji. Spectral algorithms for community detection in directed networks. *Journal of Machine Learning Research*, 21:1–45, 2020.
- Min Xu, Varun Jog, and Po-Ling Loh. Optimal rates for community estimation in the weighted stochastic block model. *Annals of Statistics*, 48(1):183–204, 2020.
- Bo Yang, William Cheung, and Jiming Liu. Community mining from signed social networks. *IEEE transactions on knowledge and data engineering*, 19(10):1333–1348, 2007.
- Wayne W Zachary. An information flow model for conflict and fission in small groups. *Journal of anthropological research*, 33(4):452–473, 1977.
- Yuan Zhang, Elizaveta Levina, and Ji Zhu. Detecting overlapping communities in networks using spectral methods. *SIAM Journal on Mathematics of Data Science*, 2(2):265–283, 2020.
- Yunpeng Zhao, Elizaveta Levina, and Ji Zhu. Consistency of community detection in networks under degree-corrected stochastic block models. *Annals of Statistics*, 40(4):2266–2292, 2012.

Zhixin Zhou and Arash A.Amini. Analysis of spectral clustering algorithms for community detection: the general bipartite setting. *Journal of Machine Learning Research*, 20(47): 1–47, 2019.

Appendix A. Vertex hunting algorithm

Algorithm 2 is the SP algorithm.

Algorithm 2 Successive Projection (SP) Gillis and Vavasis (2015)

Require: Near-separable matrix $Y_{sp} = S_{sp}M_{sp} + Z_{sp} \in \mathbb{R}_+^{m \times n}$, where S_{sp}, M_{sp} should satisfy Assumption 1 Gillis and Vavasis (2015), the number r of columns to be extracted.

Ensure: Set of indices \mathcal{K} such that $Y_{sp}(\mathcal{K}, :) \approx S$ (up to permutation)

- 1: Let $R = Y_{sp}, \mathcal{K} = \{\}, k = 1$.
 - 2: **While** $R \neq 0$ and $k \leq r$ **do**
 - 3: $k_* = \operatorname{argmax}_k \|R(k, :)\|_F$.
 - 4: $u_k = R(k_*, :)$.
 - 5: $R \leftarrow (I - \frac{u_k u_k'}{\|u_k\|_F^2})R$.
 - 6: $\mathcal{K} = \mathcal{K} \cup \{k_*\}$.
 - 7: $k = k + 1$.
 - 8: **end while**
-

Appendix B. Proofs under MMDF

B.1 Proof of Proposition 1

Proof By Lemma 1, under MMDF, $U = \Pi B = \Pi U(\mathcal{I}, :)$ gives $\Pi U(\mathcal{I}, :) = \tilde{\Pi} U(\mathcal{I}, :)$ since $\Omega = \rho \Pi \Pi' = \rho \tilde{\Pi} \tilde{\Pi}' = U \Lambda U'$. Since $\operatorname{rank}(P) = \operatorname{rank}(\tilde{P}) = \operatorname{rank}(\Pi) = \operatorname{rank}(\tilde{\Pi}) = K$ and $B \in \mathbb{R}^{K \times K}$, we have $\operatorname{rank}(B) = K$ and the inverse of B exists. Therefore $\Pi B = \tilde{\Pi} B$ gives $\Pi = \tilde{\Pi}$. Since $\Omega(\mathcal{I}, \mathcal{I}) = \rho \Pi(\mathcal{I}, :) \Pi'(\mathcal{I}, :) = \rho P = \rho \tilde{\Pi}(\mathcal{I}, :) \tilde{\Pi}'(\mathcal{I}, :) = \rho \Pi(\mathcal{I}, :) \tilde{P}'(\mathcal{I}, :) = \rho \tilde{P}$, we have $P = \tilde{P}$, and this proposition follows. ■

B.2 Proof of Lemma 1

Proof Since $\Omega = \Pi \rho \Pi' = U \Lambda U'$ and $U'U = I_K$, we have $U = \Pi \rho \Pi' U \Lambda^{-1}$, i.e., $B = \rho \Pi' U \Lambda^{-1}$. So B is unique. Since $U = \Pi B$, we have $U(\mathcal{I}, :) = \Pi(\mathcal{I}, :) B = B$ and the lemma follows. ■

B.3 Proof of Lemma 2

Proof First, we use Theorem 1.4 (the Matrix Bernstein) of Tropp (2012) to build an upper bound of $\|A - \Omega\|_\infty$. This theorem is given below

Theorem 1 Consider a finite sequence $\{X_k\}$ of independent, random, self-adjoint matrices with dimension d . Assume that each random matrix satisfies

$$\mathbb{E}[X_k] = 0, \text{ and } \|X_k\| \leq R \text{ almost surely.}$$

Then, for all $t \geq 0$,

$$\mathbb{P}(\|\sum_k X_k\| \geq t) \leq d \cdot \exp\left(\frac{-t^2/2}{\sigma^2 + Rt/3}\right),$$

where $\sigma^2 := \|\sum_k \mathbb{E}(X_k^2)\|$.

Let $x = (x_1, x_2, \dots, x_n)'$ be any $n \times 1$ vector. For any $i, j \in [n]$, we have $\mathbb{E}[(A(i, j) - \Omega(i, j))x(j)] = 0$ and $\|(A(i, j) - \Omega(i, j))x(j)\| \leq \tau \|x\|_\infty$ by Assumption 1. Set $R = \tau \|x\|_\infty$, a finite value by Assumption 1. Since $\|\sum_{j=1}^n \mathbb{E}[(A(i, j) - \Omega(i, j))^2 x^2(j)]\| = \|\sum_{j=1}^n x^2(j) \mathbb{E}[(A(i, j) - \Omega(i, j))^2]\| = \|\sum_{j=1}^n x^2(j) \text{Var}(A(i, j))\| \leq \gamma \rho \sum_{j=1}^n x^2(j)$ where the last inequality holds by Assumption 1, by Theorem 1, for any $t \geq 0$ and $i \in [n]$, we have

$$\mathbb{P}(|\sum_{j=1}^n (A(i, j) - \Omega(i, j))x(j)| > t) \leq 2\exp\left(-\frac{t^2/2}{\gamma \rho \sum_{j=1}^n x^2(j) + \frac{Rt}{3}}\right).$$

Set $x(j)$ as 1 or -1 such that $(A(i, j) - \Omega(i, j))y(j) = |A(i, j) - \Omega(i, j)|$, we have

$$\mathbb{P}(\|A - \Omega\|_\infty > t) \leq 2\exp\left(-\frac{t^2/2}{\gamma \rho n + \frac{Rt}{3}}\right).$$

Set $t = \frac{\alpha+1+\sqrt{(\alpha+1)(\alpha+19)}}{3} \sqrt{\gamma \rho n \log(n)}$ for any $\alpha > 0$. By assumption 2, we have

$$\mathbb{P}(\|A - \Omega\|_\infty > t) \leq 2\exp\left(-\frac{t^2/2}{\gamma \rho n + \frac{Rt}{3}}\right) \leq n^{-\alpha}.$$

By Theorem 4.2 of Cape et al. (2019), when $\sigma_K(\Omega) \geq 4\|A - \Omega\|_\infty$, we have

$$\|\hat{U} - U\mathcal{O}\|_{2 \rightarrow \infty} \leq 14 \frac{\|A - \Omega\|_\infty}{\sigma_K(\Omega)} \|U\|_{2 \rightarrow \infty},$$

where \mathcal{O} is a $K \times K$ orthogonal matrix. With probability at least $1 - o(n^{-\alpha})$, we have

$$\|\hat{U} - U\mathcal{O}\|_{2 \rightarrow \infty} = O\left(\frac{\|U\|_{2 \rightarrow \infty} \sqrt{\gamma \rho n \log(n)}}{\sigma_K(\Omega)}\right).$$

Since $\hat{U}'\hat{U} = I_K, U'U = I_K$, by basic algebra, we have $\|\hat{U}'\hat{U}' - UU'\|_{2 \rightarrow \infty} \leq 2\|\hat{U} - U\mathcal{O}\|_{2 \rightarrow \infty}$, which gives

$$\|\hat{U}'\hat{U}' - UU'\|_{2 \rightarrow \infty} = O\left(\frac{\|U\|_{2 \rightarrow \infty} \sqrt{\gamma \rho n \log(n)}}{\sigma_K(\Omega)}\right).$$

Since $\sigma_K(\Omega) \geq \sigma_K(P)\rho\lambda_K(\Pi'\Pi)$ by Lemma II.4 of Mao et al. (2020) and $\|U\|_{2 \rightarrow \infty}^2 \leq \frac{1}{\lambda_K(\Pi'\Pi)}$ by Lemma 3.1 of Mao et al. (2020), where this two lemmas are distribution-free and always hold as long as Eqs (2), (4) and (5) hold, we have

$$\|\hat{U}\hat{U}' - UU'\|_{2 \rightarrow \infty} = O\left(\frac{\sqrt{\gamma n \log(n)}}{\sigma_K(P)\rho^{0.5}\lambda_K^{1.5}(\Pi'\Pi)}\right).$$

Set $\alpha = 3$, and this claim follows. ■

B.4 Proof of Theorem 1

Proof Since DFSP is the SPACL algorithm without the prune step of Mao et al. (2020), the proof of DFSP's consistency is same as SPACL except the row-wise eigenspace error step where we need to consider γ which is directly related with distribution \mathcal{F} . By Eq (3) in Theorem 3.2 of Mao et al. (2020) where the proof is distribution-free, there exists a $K \times K$ permutation matrix \mathcal{P} such that

$$\max_{i \in [n]} \|e'_i(\hat{\Pi} - \Pi\mathcal{P})\|_1 = O(\varpi\kappa(\Pi'\Pi)\sqrt{\lambda_1(\Pi'\Pi)}).$$

■

B.5 Proof of Corollary 1

Proof When $\lambda_K(\Pi'\Pi) = O(\frac{n}{K})$ and $K = O(1)$, we have $\max_{i \in [n]} \|e'_i(\hat{\Pi} - \Pi\mathcal{P})\|_1 = O(\varpi\sqrt{n})$ by Theorem 1, and $\varpi = O(\frac{1}{\sigma_K(P)} \frac{1}{\sqrt{n}} \sqrt{\frac{\gamma \log(n)}{\rho^n}})$ by Lemma 2. Then the corollary follows immediately. ■